Functional Heterogeneity of Mammalian IFITM Proteins against HIV-1

Federico Marziali, Mathilde Delpeuch, Anuj Kumar, Romain Appourchaux, Jérémy Dufloo, Kevin Tartour, Lucie Etienne, Andrea Cimarelli

Functional heterogeneity of mammalian IFITM proteins against HIV-1

Federico Marziali, Mathilde Delpeuch, Anuj Kumar, Romain Appourchaux, Jérémy Dufloo[1], Kevin Tartour[2], Lucie Etienne, Andrea Cimarelli§

Centre International de Recherche en Infectiologie (CIRI)
Univ Lyon,
Inserm, U1111,
Université Claude Bernard Lyon 1,
CNRS, UMR5308,
ENS de Lyon,
46 Allée d'Italie-69007 Lyon-France

Running title: IFITM functional heterogeneity against HIV

1. Present address: Institut Pasteur, Paris, France
2. Present address: IGFL, Lyon, France

§ Correspondent footnote: correspondence should be addressed to Andrea Cimarelli, CIRI, 46 Allée d'Italie, 69364 Lyon, France. E-mail: acimarel@ens-lyon.fr

Keywords: IFITM, Interferon, HIV, virus, innate immunity, restriction factor

ABSTRACT

IFITMs are a family of interferon-inducible proteins that inhibit a broad range of viruses by interfering with viral to cellular membrane fusion. The antiviral activity of IFITMs is highly regulated by several post-translational modifications and by a number of protein domains that modulate steady-state protein levels, trafficking and antiviral effectiveness.

Taking advantage of the natural diversity existing among IFITMs of different animal species, we have compared twenty-one IFITMs for their ability to inhibit HIV-1 at two steps: during virus entry into cells (target cell protection) and during the production of novel virion particles (negative imprinting of virion particles' infectivity).

We found a high functional heterogeneity among IFITM homologs with respect to both antiviral modalities, with IFITM members that exhibit enhanced viral inhibition, while others have no ability to block HIV-1. These differences could not be ascribed to known regulatory domains and could only be partially explained through differential protein stability, implying the existence of additional mechanisms. Through the use of chimeras between active and inactive IFITMs, we demonstrate that the cross-talk between distinct domains of IFITMs is an important contributor of their antiviral potency. Finally, we identified murine IFITMs as natural variants competent for target cell protection, but not for negative imprinting of virion particles' infectivity, suggesting that the two properties may, at least in principle, be uncoupled.

Overall, our results shed new light on the complex relationship between IFITMs and viral infection and point to the cross-talk between IFITM domains as a novel layer of regulation of their activity.

AUTHOR SUMMARY

IFITMs are broad viral inhibitors capable of interfering with both early and late phases of the replicative cycle of many different viruses. By comparing twenty-one IFITM proteins issued from different animal species for their ability to inhibit HIV-1, we have identified several that exhibit either enhanced or impaired antiviral behavior. This functional diversity is not driven by differences in known domains and can only be partly explained through differential protein stability. Chimeras between active and inactive IFITMs point to the cross-talk between individual IFITM domains as important for optimal antiviral activity. Finally, we show that murine IFITMs are not capable of decreasing the infectivity of newly-produced HIV-1 virion particles, although they retain target cell protection abilities, suggesting that these properties may be in principle disconnected.

Overall, our results shed new light on the complex layers of regulation of IFITM proteins and enrich our current understanding on these broad antiviral factors.

INTRODUCTION

The interferon-induced transmembrane proteins (IFITMs) are a family of membrane-bound proteins that play an important role in innate immune responses, due to an exquisite ability to inhibit a large spectrum of viruses (1).

Members of this family present a highly similar structural organization characterized by an intramembrane domain (IMD, previously referred to as TM1), an intracellular loop (CIL), a transmembrane domain (TMD, previously referred to as TM2) and N and C-termini of variable length and regulatory functions (2, 3, 4).

By virtue of this organization, IFITMs are localized in endo-lysosomal vesicles, plasma membrane and Golgi, and display a heterogeneous distribution influenced by both membrane dynamics and specific protein domains. As such, while the intracellular distribution of human IFITM1 is skewed towards the plasma membrane, the presence of endocytic signals at the longer N-terminus of human IFITM2/3 confer them an higher endosomal/lysosomal localization (5–8) (9, 10)(11).

IFITMs present at least two peculiar features that distinguish them from many antiviral factors. First, they can inhibit a broad spectrum of viruses. Second, by acting on viral-to-cellular membrane fusion, they can interfere with two distinct phases of the replicative cycle common to most viruses: (i) during the step of virus entry in target cells (property defined as target cell protection and historically the first associated to IFITM inhibition (2, and reviewed in 4), and (ii) by triggering the production of novel virion particles of decreased infectivity (property that we refer to as the negative imprinting of virion particles' infectivity, 12–15).

In target cells, very recent studies have visually shown how IFITMs lead to the sequestration

of incoming virion particles in endosomes and enhance their trafficking to lysosomes for degradation (17–19).

Instead, in infected cells undergoing active virion production, IFITMs lead the production of novel virion particles that incorporate IFITMs and exhibit decreased infectivity (13–15, 20). Although whether the physical incorporation of IFITMs in virion particles is required for this effect remains to be formally demonstrated, the presence of IFITMs during the virion assembly process leads to virions with a reduced propensity to undergo membrane fusion, similarly to what has been described during infection of target cells (14, 15, 19, 21–23), as well as in more recent functions associated to the biology of IFITMs (24–26). In the case of target cell protection, the membrane fusion defect has been proposed to be due to the direct rigidification of membranes in which IFITMs are inserted and oligomerize (21, 23, 27). Whether the same mechanism applies to membrane fusion inhibition in IFITM-containing virion particles remains unclear.

IFITMs are regulated by numerous post-translational modifications (palmitoylation, methylation, phosphorylation and ubiquitination) that control their intracellular levels, their pattern of distribution in cells and ultimately their antiviral activities (5, 6, 10). In this respect, human IFITM2 and IFITM3 exhibit long N-termini containing two juxtaposed regulatory domains: a PPxY domain that serves as a docking site for the E3-ubiquitin ligase neural precursor cell expressed developmentally down-regulated protein 4 (NEDD4) and a Yxxϕ domain (where ϕ stands for bulky amino acid residues) that directs Adaptor protein 2 (AP2) complex-mediated endocytosis (5, 6, 10) and these activities can be modulated by the kinase Fyn through phosphorylation of the tyrosine residue common to both domains (5, 28). In contrast, relatively little is known about regulatory domains in human IFITM1 that lacks the

above-mentioned domains due to a shorter N-terminus and possesses instead a longer C-terminal tail. A single study reported the existence of a non-canonical dibasic sequence (KRxx) at the IFITM1 C-terminus that triggers AP3-mediated endocytosis and lysosomal targeting (8). This domain appears however unique to human IFITM1.

While several studies have examined the antiviral properties of individual animal IFITM molecules (albeit essentially during target cell protection) (29–35)(11), none has so far compared the antiviral properties of a large number of animal IFITMs in a single homogeneous setup, comparison that may reveal differences in terms of species specificity and that may point to IFITM domains involved in protein stability, intracellular distribution, antiviral potency and so forth.

Using a homogeneous setting, we have compared here 21 different animal IFITM proteins for their antiviral activities against HIV-1 in human cells in terms of target cell protection and negative imprinting of virion particles. Our findings highlight a remarkable heterogeneity in the action of these proteins against HIV-1, with homologs that have either completely lost their ability to inhibit the virus, while others on the contrary can do it more efficiently. The antiviral activities of the different IFITMs cannot simply be ascribed to the presence or absence of known regulatory domains in the N terminus of IFITMs that clearly distinguish IFITM2/3 molecules from IFITM1s and it can only be partially explained through protein stability, suggesting the existence of additional layers of regulation. The phenotype of chimeras obtained between antiviral and non-antiviral IFITMs highlights the importance of a cross-talk between individual domains for optimal antiviral activity. Finally, while past results from our lab failed to dissociate the two antiviral properties ascribed to IFITMs (20), we herein identify murine IFITMs as molecules intrinsically deficient in their ability to

mediate the negative imprinting of HIV-1 virions, while maintaining their effect during target cell protection. Thus, these results indicate for the first time that these two properties may be, at least in principle, uncoupled.

RESULTS

Description of the mammalian IFITMs used in this study. To benefit from the natural variability existing among IFITMs, twenty different IFITM proteins derived from a wide range of mammalian species were selected, based on cells availability and successful cloning and compared to an identically HA-tagged human IFITM3 (H3), the antiviral functions of which have been well characterized with respect to HIV-1 (Fig. 1A) (14–16, 36, 37). For clarity's purposes, the *IFITM* genome reference nomenclature was maintained, despite the caveat that this may be misleading, because some are from poorly annotated genomes and *IFITM* gene family annotations do not follow its evolutionary history. Two referenced *IFITM1-like* genes were also included in our analysis (*Canis Lupus*, D (dog), D1La and D1Lb), along with murine (*Mus musculus*, M) *IFITM6* and *IFITM7* (Fig. 1A for a schematic representation of the genomic organization of *IFITMs* used here). At a general level, the percentage identity across the mammal IFITMs analyzed here was high with a minimum of 50% for the most divergent members (M6 and M7) (Fig. 1B, for alignment purposes human IFITM1 and IFITM2 were also included). A major difference between human IFITM1 and IFITM2/3 is the presence in the former of a shorter N-terminus devoid of regulatory sequences that play important roles in IFITM trafficking and stability and of a longer C terminus that contributes to its antiviral properties, at least in human IFITM1.

A simple survey of the lengths of the N and C termini among the mammalian IFITMs tested here indicates that while the N-terminus appears homogeneous in IFITM2/3-like and IFITM1-like members (53 to 55 and 31-32 amino acids, respectively), the C-terminus varies to a greater extent from 1 amino acid in M1 to 18 in M2 (Fig. 1C). In addition, a number of IFITM molecules present combinations of either long N and C termini (B3, P2 and P3, M2, D3, C3 and G3) or short N and C ones (M1 and R1).

All IFITM2/3-like members exhibited the adjacent PPxY and YxxΦ domains important for NEDD4 and AP2 recruitment respectively (6, 28), with the sole exception of the rabbit IFITM3 protein (R3) that presented only the former. Lastly, while the Nter regions of mammalian IFITMs present enough homology to allow their good alignment, the Cter regions exhibit very little sequence homology between the selected species (Fig. 1C).

Next, the intracellular distribution of the different IFITMs was examined by confocal microscopy upon ectopic transfection in HEK293T cells (Fig. 2). Several IFITMs exhibited a punctuate intracellular staining similar to H3 (B3, P2, P3, M2, M3, M6, G3, D3), in some cases marked by accrued perinuclear accumulation (C3, R3 and to a lower measure M7) compatible with their accumulation in the Golgi. Instead, higher plasma membrane distribution was observed for the remaining members (B1, B2, P1, M1, D1 and D1La, D1Lb, C1 and R1). Overall, the different IFITM proteins display a heterogeneous distribution skewed towards either the plasma membrane or internal membranes, as described for their human counterparts (4, 20). The only exception was B2 that, despite its nomenclature, displays both an IFITM1-like plasma membrane distribution and sequence features.

Mammalian IFITMs display a heterogeneous behavior with respect to their ability to protect target cells from infection and to negatively imprint HIV-1 virion particles infectivity. To date, animal IFITM antiviral activities have been mostly evaluated in homologous host-species-virus settings; i.e. in cells of the same species and against viruses specific for that species (29, 30, 38–41), making a direct comparison of their antiviral potency difficult. Here, we aimed at comparing the antiviral behavior of the different IFITMs in a single cellular setting and to this end, both target cell protection and negative imprinting of virion's infectivity abilities of the different IFITMs were assessed against HIV-1. Target cell protection was evaluated by challenging CD4/CXCR4- HEK293T cells expressing the different IFITMs with a NL4-3-Envelope HIV-1 GFP-coding virus, prior to flow cytometry analysis two days post-infection (Fig. 3A). Negative imprinting of virion particles was determined by producing HIV-1 viruses in cells expressing the different IFITMs and by using purified and normalized amounts of virion particles to challenge target cells (Fig. 3A). Transfections were carried out with DNA levels that allowed a comparable IFITM expression with IFN-stimulated primary cells, at least as appreciated for human IFITMs, as precedently described in (14, 20). The same DNA levels were then used for the remaining IFITM orthologs. Upon ectopic expression, the steady-state levels of the different IFITMs varied considerably following WB analyses with few members either barely detectable or detectable only upon overexposure (as M6, M7 and D3, Fig. 3B and see below Fig. 4 for a quantification by intracellular flow cytometry). In the case of HIV-1 virions produced in the presence of IFITMs, the levels of virion-associated IFITM proteins mirrored their intracellular levels of expression, in agreement with our previous mutagenesis study conducted on human IFITM3 (14, 20). As we and others already documented (14–16, 20), IFITM expression exerted a

minor but detectable effect on the extent of virion released (Fig. 3B), so that subsequent experiments made use of exo-RT normalized virions.

Under the conditions used here, H3 expression in target cells induced a two-fold protection of cells from HIV-1 infection (Fig. 3C, white bars for target cell protection results). Several mammalian IFITMs exhibited antiviral activities comparable to the ones of H3 (in particular B3, P1, M2, M3, G3 and R3), while others displayed enhanced inhibitory capacities (ten-fold reduction for B1, B2, D1La and R1; four to eight-fold reduction for P2, P3, M1 and D1Lb). Interestingly, several IFITMs were found to display no discernable antiviral effect during target cell protection (C1, C3, D1, D3, M6 and M7). While this could be foreseen for the most divergent IFITM members (specifically M6 and M7 that no data has so far linked to IFN responses), the lack of antiviral activities in the remaining IFITM members was unexpected.

Next, the different IFITMs were tested for their ability to alter the infectivity of normalized HIV-1 virions (Fig 3C, blue bars). As expected, H3 drove the production of virions exhibiting a three-fold decrease in infectivity over a single round of infection assay. In addition, several IFITMs behaved as H3 (B2, B3, P1, P2, P3, D1La, R1 and R3). In stark contrast, a more drastic phenotype (six to ten-fold reduction in infectivity) was observed for B1, G3 and D1Lb, while no antiviral activity was detected for C1, C3, D1, D3, M1, M2, M3, M6 and M7. Lastly, the expression of M2, M6 and D3 exerted a positive effect on the infectivity of virion particles.

At a general level, a strong positive correlation was observed between the ability of individual IFITMs to interfere with the infectivities measured in target cell protection and negative imprinting of virions (Fig 3D; $R=0,77$, p-value<0.0001), suggesting a strong interdependence

between these two activities, as previously suggested (20). The only exceptions were noted in murine IFITMs M1, M2 and M3 proficient in target cell protection, but lacking detectable effects on the infectivity of newly-formed HIV-1 virions. Overall, the results obtained here highlight the heterogeneous behavior of animal IFITMs with respect to their antiviral properties, as assessed in a unique cellular and viral setting.

The intracellular levels of the different mammalian IFITMs is an important, but not unique parameter of their antiviral properties.

The antiviral potency of IFITM proteins is influenced by a number of factors and among them those governing the protein's steady-state levels (6, 11, 16, 20). To determine whether protein stability (at least at steady state), could relate to the antiviral behavior of the IFITMs examined here, we used intracellular staining and flow cytometry analysis (Fig. 4A for representative panels and 4B for cumulative data). When thus analyzed and compared to human IFITM3, the intracellular levels of accumulation of IFITMs varied from 2-fold higher to 4-fold lower. Variations spanned animal clade division in that IFITMs within one species could present increased or decreased steady state levels. The intracellular levels of IFITM expression (as assessed by the mean fluorescent intensity, MFI) was inversely correlated with the infectivities measured in both target cell and negative imprinting, indicating that IFITMs present at higher levels were generally more antiviral (Fig. 4C, $r=-0.7601$; $p=0.0001$ and $r=-0.54$; $p=0.01$, respectively). This correlation was however lower for the negative imprinting of virion particles defect, indicating that this property is less reliant on the levels of IFITMs in cells, than target cell protection. Overall, this analysis indicates that protein stability at steady state is an important parameter of the antiviral properties of IFITMs in agreement with data present in the literature.

To assess the contribution of protein levels to the lack of antiviral activity during target cell protection, property more influenced by the intracellular levels of IFITMs, increasing doses of D1 and C1 were used in a comparison with other IFITMs exhibiting antiviral activity (D1Lb and R1, respectively). To this end, target cells transfected with different amounts of IFITM-coding DNAs were challenged with WT HIV-1, prior to flow cytometry analysis two days later (Fig. 5A). Protein levels were quantified by densitometry following WB, as this yielded similar results than intracellular staining and flow cytometry analyses, under the conditions used here.

Increasing doses of D1 did not significantly alter virion infectivity and when D1 was expressed at similar levels than D1Lb the different antiviral behavior was still significant (Fig. 5A). A similar behavior was observed upon the expression of increasing doses of C1, although in this case we were unable to achieve a notable increase in C1 protein levels. To circumvent this issue, we used a reciprocal setup in which a fixed dose of C1 was compared to decreasing levels of R1 (Fig. 5B). In this case, despite the fact that the antiviral activity of R1 was gradually lost upon dilution, R1 was still able to inhibit viral infection when expressed at similar levels than C1. Altogether, these results indicate that protein stability is important, but is not the sole contributor of the observed differences in the antiviral behavior of IFITMs.

Elements described as crucial for IFITM antiviral activities are largely conserved among mammalian IFITMs. To investigate potential amino acid differences or evolutionary paths between the mammalian IFITMs with and without antiviral activities, we

performed comparative genetic and phylogenetic analyses. Benefiting from the natural variations existing among mammalian IFITMs, we grouped members according to their non-antiviral (C1, D1, C3 and D3, only members devoid of both antiviral activities were grouped here) and antiviral (the remaining ones) behavior, omitting M6 and M7 from the analysis due to their higher divergence (Fig. 6A and 6B). No single common amino acid change was able to discriminate IFITMs according to their antiviral behavior. Indeed, most IFITM members displayed three conserved cysteines (C71, 72, 105; amino acid positions relative to H3) important for palmitoylation and membrane association (7, 42), with the exception of C71 replaced by phenylalanine in antiviral D1La and D1Lb IFITMs. Most IFITMs also displayed four conserved phenylalanines (F63, F67, F75, F78) reported as relevant for antiviral functions (43, 44), Residues F75 and F78 were previously proposed to mediate IFITM3 oligomerization, but this was not the case when examined in living cells (45) (46). Therefore, these four phenylalanines are important functional determinants for unknown reasons. The only exceptions found in our analysis were the F75 and F78 residues that were replaced by isoleucine and tyrosine in C1 and M1, M2 and M3, respectively. Moreover, IFITMs possess several lysines that can be ubiquitinated, one specific to the long Nter of IFITM2/3-like proteins and three others shared by all IFITMs (K83, K88 and K104) (6, 47). Of these, K83 and K88, but not K104 were strictly conserved among mammalian IFITMs, despite the fact that ubiquitination of K104 together with K83 is required for a recently-identified scaffolding property of IFITM3 involved in B cell signaling (26). Remarkably, in none of the positions mentioned above and described in the literature to modulate the antiviral properties of IFITMs a strict correlation existed between antiviral and non-antiviral IFITMs. Furthermore, residues described as forming an amphipathic helix in the IMD of human IFITMs (VWSLFNTL/I/VF) (48), as well as a very recently identified GxxxG motif with crucial

297 relevance in membrane rigidification (27), were also conserved among all mammalian
298 IFITMs tested. Finally, the "non-antiviral" IFITMs did not group together on a phylogenetic
299 analysis (Fig. 6C), suggesting that they do not share a common ancestor and that the absence
300 of antiviral activity is not due to an ancient single event.
301 Therefore, the main elements previously described as crucial for the antiviral activity of
302 IFITMs are largely conserved among mammalian IFITMs, indicating that additional ones are
303 likely to contribute to the fine regulation of their overall antiviral behavior.
304
305 **Chimeras between active and inactive IFITM homologues highlight the importance of**
306 **the cross-talk between individual domains to finely tune antiviral behavior.** To identify
307 the domain(s) at the basis of the distinct behavior of the different IFITMs, we generated
308 chimeric IFITM proteins in which domains of the antiviral R1 were inserted into the non-
309 antiviral C1 either individually, or in combination (Fig. 7A). Contrarily to other individual
310 domains, the Cter of R1 (C1-C_{R1}) promoted a substantial increase in protein accumulation at
311 steady state and its combination with the TMD domain (C1-$(TMD+C)_{R1}$) further increased
312 it (Fig. 7B and 7C). The different chimeras did not exhibit gross changes in their intracellular
313 distribution after confocal microscopy analysis, with the exception of the C1-TMD_{R1} chimera
314 that appeared to have lost the plasma membrane distribution typical of IFITM1-like proteins
315 (Fig. 7D). Interestingly, when cells expressing the different chimeras were challenged with
316 HIV-1 in target cell protection, a single chimera was able to exhibit significant antiviral
317 activity (C1-$(TMD+C)_{R1}$, Fig. 7E), indicating the importance of the cross-talk between the
318 TMD and the Cter domains for the antiviral activity.

A similar approach was used to engineer chimeras between D1 and D1Lb, respectively inactive and active against HIV-1 (Fig. 8A). Also in this case, the Cter of D1Lb (D1-C_b) was able to substantially rescue the low protein expression levels of D1. However, in this case it was the combination of the Cter with the Nter domains (D1-$(N+C)_b$) that yielded the highest increase in protein levels (Fig. 8B and 8C). No gross modifications of the intracellular distributions of the different chimeras were observed with the exception of the D1-C_b and the D1-$(TMD+C)_b$ chimeras that exhibited higher perinuclear accumulation than WT (Fig. 8D). When the chimeras were tested for their ability to mediate target cell protection against HIV-1, we again found that the cross-talk between the TMD and the Cter was important for the antiviral activity (Fig. 8E). Interestingly, in this case the combination between the Nter and the IMD domains was also important to restore full antiviral activities. These results indicate that cross-talks between individual domains are important for optimal antiviral activity with the combination between the TMD and the Cter being important for both chimeric configurations examined, while the one between Nter with IMD and Cter with TMD being important only in the case of the D1/D1Lb chimera.

Finally, the antiviral chimeras were also tested for their ability to mediate the negative imprinting of virion particles infectivity. For this, HIV-1 virions produced in cells ectopically expressing the IFITMs were used to challenge target cells (Fig. 9A for a schematic presentation of the chimeras and the experimental setup). All chimeric forms of IFITMs decreased HIV-1 virions´ infectivity, with C1-$(TMD+C)_{R1}$ exerting an antiviral effect largely comparable to the parental R1 homologue and the D1-$(N+IMD)_b$ and D1-$(TMD+C)_b$ chimeras still antiviral despite the fact that the latter appeared less potent than D1Lb (Fig.

9B). Hence, the domain crosstalks showed above as relevant for target cell protection activity plays an important role also during negative imprinting of virions infectivity.

Murine IFITM3 is a natural IFITM variant devoid of negative imprinting of HIV-1 virion particles ability. An important result highlighted from our study is the fact that despite being proficient in target cell protein, murine IFITM 1, 2 and 3 seem not to affect the infectivity of newly-produced HIV-1 virion particles. To determine whether this could be dependent on insufficient levels of expression, HIV-1 virions were produced in the presence of increasing doses of M3, prior to virion normalization and challenge of target cells. Even under conditions of increased doses of M3 (Fig. 10A), a consistent lack of antiviral effects was noted suggesting a true deficiency in negative imprinting of HIV-1 virion's infectivity, at least under the experimental conditions used here.

As mentioned above, we noticed that F78 (numbering with respect to human IFITM3, see Fig 6) is commonly substituted by tyrosine in murine IFITMs (M1, M2 and M3) that lack negative imprinting of virion particles abilities. As such, we substituted this residue back to phenylalanine (Y78F) in the context of M3 and tested its ability to impair the infectivity of newly-produced virion particles, using the same experimental setup. However, no change in infectivity could be measured when virion particles were produced in the presence of increasing levels of the M3 Y78F mutant (Fig. 10B), indicating that this residue does not play an important role in this setting.

Overall, these results indicate that murine IFITM3 is a natural variant impaired in their ability to negatively imprint the infectivity of newly-produced virion particles, at least in the case of HIV-1 and also further highlight that protein stability is not the sole contributor of the observed differences in the antiviral behavior of IFITMs.

DISCUSSION

In this study, we have taken advantage of the natural variability existing between a large panel of mammalian IFITMs to compare their potency against HIV-1 in a single experimental system through expression in human cells. In doing so, we have uncovered IFITM homologs that exhibit either enhanced, or completely absent, ability to affect both target cell protection and negative imprinting of HIV-1 virions infectivity. Interestingly despite few exceptions, the domains described in previous studies as important for either post-translational modifications, multimerization or overall antiviral properties are conserved across all the IFITMs tested here independently of their antiviral behavior, pointing to the existence of additional determinants for the antiviral activities of IFITMs. In this respect, the results obtained with our chimeras indicate that one such determinant may be the cross-talk between individual IFITM domains.

A general distinction between human IFITM1 and IFITM2/3 proteins is the reciprocal presence of long C and N termini, respectively. Long Nter are indeed well maintained in mammalian IFITM2/3 that also exhibit a strict conservation of the NEDD4 and AP2 recruitment domains with one sole exception (R3). However, the Cter appears more heterogeneous, and long C-termini are in some cases present in combination with long Nter in IFITM2/3 molecules (B3, P1, P2, M3, D3, C3 and G3). Whether this latter endows such molecules with additional regulatory features with respect to those described for their human counterparts remains unknown. Relatively few studies have examined the functions of the Cter of IFITM proteins and have been essentially focused on human IFITM1 in which a

388 regulatory dibasic KRxx domain has been shown to regulate association to AP3 (8).
389 However, this domain is absent in all the remaining IFITMs, so that how and whether the
390 Cter regulates more commonly the behavior and properties of IFITM1-like proteins remain
391 unclear. In this respect, it is of interest that M1 and R1 present very short N and C-termini
392 which may indicate them as *core* minimal IFITM homologs devoid of some of the multiple
393 regulatory possibilities described for other IFITMs.

394 It is evident from our comparative analysis that no common specific residue or described
395 domain can discriminate active from inactive IFITMs. A recent report highlighted the
396 importance of the polymorphism of residues (P/W/T/F/Y) in the rates of palmitoylation on
397 adjacent cysteines (C71/C72) and in the restriction capacity of bat IFITMs (33) and another
398 determined the functional relevance of a polymorphism within the AP2 binding site of
399 African green monkeys IFITM3 alleles (I22) (49). While variations at these residues do not
400 explain the antiviral behavior of the IFITM tested here, these findings raise the possibility
401 that additional polymorphism may finely tune IFITM functions, possibly in a species-specific
402 context.

403 Previous work from a number of laboratories including ours has highlighted the importance
404 of the intracellular levels of accumulation for the antiviral effects of human IFITM3 (14–16,
405 20, 36). However, the results obtained with two non-antiviral IFITM proteins (C1 and D1),
406 as well as with chimeras clearly indicate that protein levels are not the sole determinant of
407 antiviral behavior, pointing to the existence of additional layers of regulation.

408 With the caveat that we have not examined the dynamic distribution of the different IFITMs
409 and that for a given mutation it is difficult to completely separate effects on protein levels
410 from those on antiviral behavior, the results we have obtained with two sets of chimeras
411 indicate that the cross-talk between two distinct domains (in particular the TMD and the Cter)

412 is an important modulator of antiviral functions. While the Cter and TMD domains in R1 are
413 very different from those in C1, they exhibit only four and five amino acid changes between
414 D1 and D1Lb, respectively. Yet, the transfer of the Cter and TMD domains is sufficient to
415 restore antiviral functions. The fact that the combination of Nter and Cter can also exert
416 similar effects in the context of the D1/D1Lb but not of the C1/R1 chimera suggests that such
417 cross-talks are likely to be different according to the specific IFITM examined, probably as
418 a result of species-specific adaptations.
419
420 At present the reasons for the absence of antiviral activities by some IFITM molecules remain
421 unclear and, in terms of evolution, it is entirely possible that this has resulted from a loss of
422 antiviral activity that has been compensated by other IFITM members of a given species not
423 tested here. However, an alternative, and not mutually exclusive, possibility we favor is that
424 certain IFITMs may be subjected to host species-specific regulation and/or exhibit optimal
425 activity against viruses naturally encountered in the same species. In this respect, the feline
426 C1 and C3 IFITMs examined here are poorly expressed in human cells and inactive against
427 HIV-1, but they may exhibit better stability and antiviral properties in a feline cell-virus
428 context.
429 To support this contention, it is interesting to note that murine IFITMs (M1, M2 and M3)
430 were found in this study to inhibit HIV-1 during target cell protection, but not to alter the
431 infectivity of newly-formed HIV-1 virion particles. While on one hand this finding is
432 important because it suggests for the first time that these two properties may be dissociated,
433 on the other it raises the possibility that murine IFITM3 may have been optimized for activity
434 against viruses of its own species. The latter would be in agreement with a recent study
435 reporting that murine IFITM3 is capable of interfering with the production of infectious

virion particles of the murine leukemia virus (MLV) (50). Thus, these results highlight the possibility that species-specific adaptations may have shaped the optimal antiviral activity of a given IFITM against viruses of the same species.

In conclusion, our study highlights a broad functional heterogeneity among mammalians IFITMs against HIV-1 and indicates that the cross-talk between IFITM domains finely tunes the antiviral properties of the different IFITMs, adding a novel layer of complexity to the regulation of the activities of these broad antiviral factors.

MATERIAL AND METHODS

Cell culture, plasmids and antibodies. HEK293T epithelial cell line ATCC (CRL-3216) and HeLa P4/P5 expressing the CD4 receptor along with the CXCR4 and CCR5 co-receptors were cultured in complete DMEM supplemented with 10% FCS. IFITMs were amplified by PCR from cDNAs obtained from relevant animal cell lines (cell lysates were kind gifts of the CelluloNet facility of the SFR-Biosciences in Lyon Gerland or of Frederick Arnaud at the IVPC, Lyon, France): MBDK, *Bos Taurus*; PK(15), *Sus scrofa*; RK15, *Oryctolagus cuniculus*; TIGMEC, *Capra hircus*; CRFK, *Felis catus*. Murine and canine IFITMs were obtained by gene synthesis (Genewiz). All IFITMs were cloned as BamH1/NotI fragments into a pcDNA-HA vector. The species abbreviations used in this manuscript are: H= *Homo sapiens*; M= *Mus musculus*; G= *Capra hircus*; D= *Canis lupus familiaris*; C= *Felis catus*; P= *Sus scrofa*; B= *Bos Taurus*; R= *Oryctolagus cuniculus*. Retrieved sequences were strictly identical to the following gene ID numbers: H3, 10410; M1, 68713; M2, 80876; M3, 66141; M6, 213002; M7, 74482; G3, 102180655; D1, 483397; D1La, 475935; D1Lb, 483396; D3,

606890; C1, 101086846; C3, 101100838; P1, 100127358; P2, 100620056; P3, 100518544; B1, 353510; B2, 615833; B3, 777594; R1, 103347593; R3, 100353245. D1/D1Lb and C1/R1 chimeras were obtained by gene synthesis (Genewiz). CD4, CCR5 and CXCR4-coding plasmids were obtained from the AIDS Reagent and Reference Program of the NIH (cat. Numbers: 158, 3325, 3326, respectively, respectively). The anti-HA (H3663) and anti-α-Tubulin (T8203) antibodies were purchased from SIGMA. The anti-HIV-1 Gag and anti-HIV-1 Env antibodies were similarly obtained from the AIDS Reagent and Reference Program of the NIH (clone 183-H5C and cat. number 288, respectively).

Virus production, purification, normalization and infections. Standard single-round of infection vectors were produced by transient calcium phosphate transfection with DNAs coding for: a mini viral genome bearing GFP (pRRL-CMV-GFP); the Gag and Gag-Pol structural proteins (8.2); the NL4-3 Env and the HIV-1 Rev protein (Rev) (4:4:1 and 0.5 μg respectively for a 10cm plate), as described in (13, 14).

The target cell protection properties of the different IFITMs were assessed by using the above-mentioned virus at a multiplicity of infection (MOI) comprised between 0.1 and 0.2 on HEK293T cells ectopically transfected thirty-six hours earlier with DNAs coding CD4, CXCR4 and the different IFITMs (0.2: 0.2 and 1 μg, respectively).

To assess the negative imprinting of virion infectivity abilities of IFITMs, HIV-1-derived lentiviral particles were produced in the presence of IFITMs by calcium phosphate DNA co-transfection of HEK293T cells using Gag-Pro-Pol, viral GFP genome, Env, Rev and IFITMs or pcDNA control plasmid (using 4: 4: 0.5: 0.5: 3 μg each for a 10-cm dish plate), as previously described (13, 14, 20). We have already shown that in the case of human IFITMs,

these levels were similar to those observed for the endogenous form in primary dendritic cells stimulated with type I interferon.

In this case, forty-eight hours after transfection, cell-free supernatants were syringe-filtered (0.45 μm) and virion particles were purified by ultracentrifugation through a 25% sucrose cushion (w/v) for two hours at 110.000g. Virion pellets were then resuspended in PBS for further analyses and normalized by exogenous-reverse transcriptase (exo-RT), as described. Infections were carried out on HeLaP4/P5 cells with normalized amounts of virions for 2-4 hours and the extent of infection was assessed three days later by flow cytometry.

Immunofluorescence and confocal microscopy. HEK293T cells growing on glass coverslips coated with poly-L-Lysine 0.01% were transfected with plasmids coding animal IFITMs with Lipofectamine 3000, according to the manufacturer's instructions (Invitrogen, LifeTechnologies). Twenty-four hours later, cells were fixed with PFA (3.7%), permeabilized with Triton 0.1% in PBS and incubated first with the primary anti-HA antibody overnight (at a 1/100 dilution), then with a secondary antibody conjugated to Alexa488 (Molecular Probes, LifeTechnologies; #A21202; 1/1000 dilution). Coverslips were stained with a DAPI-containing solution (1/10000 dilution in PBS) and mounted using the anti-quenching solution Fluormount G (Southern Biotech). Fluorescent confocal images were collected using a Zeiss LSM 880 AiryScan confocal microscope and pictures were analyzed with the ImageJ software.

Intracellular staining and flow cytometry analysis. HEK293T cells expressing the different IFITMs were permeabilized with the Cytofix/Cytoperm plus kit (cat: n°554715,

BD), according to the manufacturer's instructions, before incubation with a phycoerythrin-conjugated anti-HA antibody (Miltenyi Biotec, #130-092-257) and flow cytometry analysis. The mean fluorescent intensity of HA-positive cells was then determined using the FlowJo software.

Sequence analyses and phylogenetics. Sequence alignment of the various IFITMs were performed using amino acid sequences with PRANK -F with a gap rate of 0.005 and minor adjustments (51). The N-/C-termini of the selected mammalian IFITMs are highly variable (low homology) and are the result of complex evolutionary histories. They aligned very differently depending on the alignment method and gap parameters. All in all, only the central portion of IFITMs is enough homologous and can be correctly aligned. Visualization in Figure 6 was produced using Geneious (Biomatters, Inc.), with color-coding according to polarity, and logo plots. Phylogenetics in Figure 6 were performed using PhyML with JTT + G + I as a model and aLRT for node support (52, 53). The sequence alignment in fasta format and the phylogenetic tree in nwk format are available at https://doi.org/10.6084/m9.figshare.13365893 and https://doi.org/10.6084/m9.figshare.13365893, respectively.

Statistical analysis. One-Way Anova, one-tail Student t tests or Pearson's correlation coefficient were used, as indicated in the legend to figures.

Data Availability. All relevant data are within the paper.

ACKNOWLEDGMENTS

We wish to acknowledge the AIDS Reagents and Reference Program of the NIH for antibodies and plasmids cited in this manuscript and Frederick Arnaud for sharing material. We acknowledge the contribution of the flow cytometry (ANIRA-Cytométrie), microscopy (LYMIC-PLATIM) and genetic analysis (ANIRA-AGC CRB Cellulonet) platforms of SFR BioSciences Gerland Lyon Sud (UMS3444/US8).

Funding

The work described here in the laboratory of AC was supported by grants from the ANRS and Sidaction (2017-1 and 2019-1). AK and FM are post-doctoral fellows of the ANRS. AC and LE are supported by the CNRS. LE is supported by grants from amfAR (Mathilde Krim Phase II Fellowship no. 109140-58-RKHF), the ANR LABEX ECOFECT (ANR-11-LABX-0048 of the Université de Lyon, within the program Investissements d'Avenir [ANR-11-IDEX-0007] operated by the French National Research Agency), the Fondation pour la Recherche Médicale (FRM Projet Innovant no. ING20160435028), the FINOVI ("recently settled scientist" grant), the ANRS (no. ECTZ19143 and ECTZ118944), and a JORISS incubating grant. The funders had no role in study design, data collection and analysis, decision to publish, or preparation of the manuscript.

REFERENCES

1. Friedman RL, Manly SP, McMahon M, Kerr IM, Stark GR. 1984. Transcriptional and posttranscriptional regulation of interferon-induced gene expression in human cells. Cell 38:745–755.

2. Bailey CC, Zhong G, Huang I-C, Farzan M. 2014. IFITM-Family Proteins: The Cell's First Line of Antiviral Defense. Annu Rev Virol 1:261–283.

3. Liao Y, Goraya MU, Yuan X, Zhang B, Chiu S-H, Chen J-L. 2019. Functional Involvement of Interferon-Inducible Transmembrane Proteins in Antiviral Immunity. Front Microbiol 10:1097.

4. Brass AL, Huang I-C, Benita Y, John SP, Krishnan MN, Feeley EM, Ryan BJ, Weyer JL, van der Weyden L, Fikrig E, Adams DJ, Xavier RJ, Farzan M, Elledge SJ. 2009. The IFITM proteins mediate cellular resistance to influenza A H1N1 virus, West Nile virus, and dengue virus. Cell 139:1243–1254.

5. Chesarino NM, McMichael TM, Hach JC, Yount JS. 2014. Phosphorylation of the antiviral protein interferon-inducible transmembrane protein 3 (IFITM3) dually regulates its endocytosis and ubiquitination. J Biol Chem 289:11986–11992.

6. Chesarino NM, McMichael TM, Yount JS. 2015. E3 Ubiquitin Ligase NEDD4 Promotes Influenza Virus Infection by Decreasing Levels of the Antiviral Protein IFITM3. PLoS Pathog 11.

7. Yount JS, Moltedo B, Yang Y-Y, Charron G, Moran TM, López CB, Hang HC. 2010. Palmitoylome profiling reveals S-palmitoylation-dependent antiviral activity of IFITM3. Nat Chem Biol 6:610–614.

8. Li K, Jia R, Li M, Zheng Y-M, Miao C, Yao Y, Ji H-L, Geng Y, Qiao W, Albritton LM, Liang C, Liu S-L. 2015. A Sorting Signal Suppresses IFITM1 Restriction of Viral Entry. J Biol Chem 290:4248–4259.

9. Smith SE, Busse DC, Binter S, Weston S, Soria CD, Laksono BM, Clare S, Nieuwkoop SV, Hoogen BGV den, Clement M, Marsden M, Humphreys IR, Marsh M, Swart RL de, Wash RS, Tregoning JS, Kellam P. 2019. Interferon-Induced Transmembrane Protein 1 Restricts Replication of Viruses That Enter Cells via the Plasma Membrane. Journal of Virology 93.

10. Jia R, Xu F, Qian J, Yao Y, Miao C, Zheng Y, Liu S, Guo F, Geng Y, Qiao W, Liang C. 2014. Identification of an endocytic signal essential for the antiviral action of IFITM3. Cell Microbiol 16:1080–1093.

11. Compton AA, Roy N, Porrot F, Billet A, Casartelli N, Yount JS, Liang C, Schwartz O. 2016. Natural mutations in IFITM3 modulate post-translational regulation and toggle antiviral specificity. EMBO Rep 17:1657–1671.

12. Shi G, Schwartz O, Compton AA. 2017. More than meets the I: the diverse antiviral and cellular functions of interferon-induced transmembrane proteins. 1. Retrovirology 14:53.

13. Tartour K, Nguyen X-N, Appourchaux R, Assil S, Barateau V, Bloyet L-M, Burlaud Gaillard J, Confort M-P, Escudero-Perez B, Gruffat H, Hong SS, Moroso M, Reynard O, Reynard S,

584 Decembre E, Ftaich N, Rossi A, Wu N, Arnaud F, Baize S, Dreux M, Gerlier D, Paranhos-
585 Baccala G, Volchkov V, Roingeard P, Cimarelli A. 2017. Interference with the production of
586 infectious viral particles and bimodal inhibition of replication are broadly conserved antiviral
587 properties of IFITMs. PLoS Pathog 13.

588 14. Tartour K, Appourchaux R, Gaillard J, Nguyen X-N, Durand S, Turpin J, Beaumont E, Roch E,
589 Berger G, Mahieux R, Brand D, Roingeard P, Cimarelli A. 2014. IFITM proteins are
590 incorporated onto HIV-1 virion particles and negatively imprint their infectivity. Retrovirology
591 11:103.

592 15. Compton AA, Bruel T, Porrot F, Mallet A, Sachse M, Euvrard M, Liang C, Casartelli N,
593 Schwartz O. 2014. IFITM proteins incorporated into HIV-1 virions impair viral fusion and
594 spread. Cell Host Microbe 16:736–747.

595 16. Lu J, Pan Q, Rong L, He W, Liu S-L, Liang C. 2011. The IFITM proteins inhibit HIV-1 infection.
596 J Virol 85:2126–2137.

597 17. Kummer S, Avinoam O, Kräusslich H-G. 2019. IFITM3 Clusters on Virus Containing
598 Endosomes and Lysosomes Early in the Influenza A Infection of Human Airway Epithelial Cells.
599 Viruses 11.

600 18. Spence JS, He R, Hoffmann H-H, Das T, Thinon E, Rice CM, Peng T, Chandran K, Hang HC.
601 2019. IFITM3 directly engages and shuttles incoming virus particles to lysosomes. Nat Chem
602 Biol 15:259–268.

603 19. Suddala KC, Lee CC, Meraner P, Marin M, Markosyan RM, Desai TM, Cohen FS, Brass AL,
604 Melikyan GB. 2019. Interferon-induced transmembrane protein 3 blocks fusion of sensitive but
605 not resistant viruses by partitioning into virus-carrying endosomes. PLoS Pathog 15:e1007532.

606 20. Appourchaux R, Delpeuch M, Zhong L, Burlaud-Gaillard J, Tartour K, Savidis G, Brass A,
607 Etienne L, Roingeard P, Cimarelli A. 2019. Functional Mapping of Regions Involved in the
608 Negative Imprinting of Virion Particle Infectivity and in Target Cell Protection by Interferon-
609 Induced Transmembrane Protein 3 against HIV-1. Journal of Virology 93.

610 21. Li K, Markosyan RM, Zheng Y-M, Golfetto O, Bungart B, Li M, Ding S, He Y, Liang C, Lee
611 JC, Gratton E, Cohen FS, Liu S-L. 2013. IFITM Proteins Restrict Viral Membrane Hemifusion.
612 PLoS Pathog 9.

613 22. Lin T-Y, Chin CR, Everitt AR, Clare S, Perreira JM, Savidis G, Aker AM, John SP, Sarlah D,
614 Carreira EM, Elledge SJ, Kellam P, Brass AL. 2013. Amphotericin B increases influenza A virus
615 infection by preventing IFITM3-mediated restriction. Cell Rep 5:895–908.

616 23. Desai TM, Marin M, Chin CR, Savidis G, Brass AL, Melikyan GB. 2014. IFITM3 restricts
617 influenza A virus entry by blocking the formation of fusion pores following virus-endosome
618 hemifusion. PLoS Pathog 10:e1004048.

619 24. Zani A, Zhang L, McMichael TM, Kenney AD, Chemudupati M, Kwiek JJ, Liu S-L, Yount JS.
620 2019. Interferon-induced transmembrane proteins inhibit cell fusion mediated by trophoblast
621 syncytins. J Biol Chem 294:19844–19851.

622 25. Buchrieser J, Degrelle SA, Couderc T, Nevers Q, Disson O, Manet C, Donahue DA, Porrot F,
623 Hillion K-H, Perthame E, Arroyo MV, Souquere S, Ruigrok K, Dupressoir A, Heidmann T,

624 Montagutelli X, Fournier T, Lecuit M, Schwartz O. 2019. IFITM proteins inhibit placental
625 syncytiotrophoblast formation and promote fetal demise. Science 365:176–180.

626 26. Lee J, Robinson ME, Ma N, Artadji D, Ahmed MA, Xiao G, Sadras T, Deb G, Winchester J,
627 Cosgun KN, Geng H, Chan LN, Kume K, Miettinen TP, Zhang Y, Nix MA, Klemm L, Chen
628 CW, Chen J, Khairnar V, Wiita AP, Thomas-Tikhonenko A, Farzan M, Jung JU, Weinstock
629 DM, Manalis SR, Diamond MS, Vaidehi N, Müschen M. 2020. IFITM3 functions as a PIP3
630 scaffold to amplify PI3K signalling in B cells. Nature 1–7.

631 27. Rahman K, Coomer CA, Majdoul S, Ding SY, Padilla-Parra S, Compton AA. 2020. Homology-
632 guided identification of a conserved motif linking the antiviral functions of IFITM3 to its
633 oligomeric state. Elife 9.

634 28. Jia R, Pan Q, Ding S, Rong L, Liu S-L, Geng Y, Qiao W, Liang C. 2012. The N-Terminal Region
635 of IFITM3 Modulates Its Antiviral Activity by Regulating IFITM3 Cellular Localization. J Virol
636 86:13697–13707.

637 29. Smith SE, Gibson MS, Wash RS, Ferrara F, Wright E, Temperton N, Kellam P, Fife M. 2013.
638 Chicken Interferon-Inducible Transmembrane Protein 3 Restricts Influenza Viruses and
639 Lyssaviruses In Vitro. J Virol 87:12957–12966.

640 30. Wang J, Wang C-F, Ming S-L, Li G-L, Zeng L, Wang M-D, Su B-Q, Wang Q, Yang G-Y, Chu
641 B-B. 2020. Porcine IFITM1 is a host restriction factor that inhibits pseudorabies virus infection.
642 Int J Biol Macromol 151:1181–1193.

643 31. Xing H, Ye L, Fan J, Fu T, Li C, Zhang S, Ren L, Bai J. 2020. IFITMs of African Green Monkey
644 Can Inhibit Replication of SFTSV but Not MNV In Vitro. Viral Immunol
645 https://doi.org/10.1089/vim.2020.0132.

646 32. Chen S, Wang L, Chen J, Zhang L, Wang S, Goraya MU, Chi X, Na Y, Shao W, Yang Z, Zeng
647 X, Chen S, Chen J-L. 2017. Avian Interferon-Inducible Transmembrane Protein Family
648 Effectively Restricts Avian Tembusu Virus Infection. Front Microbiol 8:672.

649 33. Benfield CT, MacKenzie F, Ritzefeld M, Mazzon M, Weston S, Tate EW, Teo BH, Smith SE,
650 Kellam P, Holmes EC, Marsh M. 2019. Bat IFITM3 restriction depends on S-palmitoylation and
651 a polymorphic site within the CD225 domain. 1. Life Sci Alliance 3.

652 34. Benfield CTO, Smith SE, Wright E, Wash RS, Ferrara F, Temperton NJ, Kellam P. 2015. Bat
653 and pig IFN-induced transmembrane protein 3 restrict cell entry by influenza virus and
654 lyssaviruses. J Gen Virol 96:991–1005.

655 35. Bailey CC, Huang I-C, Kam C, Farzan M. 2012. Ifitm3 limits the severity of acute influenza in
656 mice. PLoS Pathog 8:e1002909.

657 36. Foster TL, Wilson H, Iyer SS, Coss K, Doores K, Smith S, Kellam P, Finzi A, Borrow P, Hahn
658 BH, Neil SJD. 2016. Resistance of Transmitted Founder HIV-1 to IFITM-Mediated Restriction.
659 Cell Host Microbe 20:429–442.

660 37. Ding S, Pan Q, Liu S-L, Liang C. 2014. HIV-1 mutates to evade IFITM1 restriction. Virology
661 454–455:11–24.

662 38. Blyth GAD, Chan WF, Webster RG, Magor KE. 2016. Duck Interferon-Inducible

663 Transmembrane Protein 3 Mediates Restriction of Influenza Viruses. J Virol 90:103–116.

664 39. Xie J, Bi Y, Xu S, Han Y, Idris A, Zhang H, Li X, Bai J, Zhang Y, Feng R. 2020. Host antiviral
665 protein IFITM2 restricts pseudorabies virus replication. Virus Research 287:198105.

666 40. Xu Z, Li X, Xue J, Shen L, Zheng W, Yin S, Xu J. 2020. S-palmitoylation of swine interferon-
667 inducible transmembrane protein is essential for its anti-JEV activity. Virology 548:82–92.

668 41. Zhang Y, Huang Y, Wang L, Huang L, Zheng J, Huang X, Qin Q. 2020. Grouper interferon-
669 induced transmembrane protein 3 (IFITM3) inhibits the infectivity of iridovirus and nodavirus
670 by restricting viral entry. Fish Shellfish Immunol 104:172–181.

671 42. McMichael TM, Zhang L, Chemudupati M, Hach JC, Kenney AD, Hang HC, Yount JS. 2017.
672 The palmitoyltransferase ZDHHC20 enhances interferon-induced transmembrane protein 3
673 (IFITM3) palmitoylation and antiviral activity. J Biol Chem 292:21517–21526.

674 43. John SP, Chin CR, Perreira JM, Feeley EM, Aker AM, Savidis G, Smith SE, Elia AEH, Everitt
675 AR, Vora M, Pertel T, Elledge SJ, Kellam P, Brass AL. 2013. The CD225 Domain of IFITM3
676 Is Required for both IFITM Protein Association and Inhibition of Influenza A Virus and Dengue
677 Virus Replication. Journal of Virology 87:7837–7852.

678 44. Zhao X, Sehgal M, Hou Z, Cheng J, Shu S, Wu S, Guo F, Marchand SJL, Lin H, Chang J, Guo
679 J-T. 2018. Identification of Residues Controlling Restriction versus Enhancing Activities of
680 IFITM Proteins on Entry of Human Coronaviruses. Journal of Virology 92.

681 45. Rahman K, Coomer CA, Majdoul S, Ding SY, Padilla-Parra S, Compton AA. 2020. Homology-
682 guided identification of a conserved motif linking the antiviral functions of IFITM3 to its
683 oligomeric state. Elife 9.

684 46. Winkler M, Wrensch F, Bosch P, Knoth M, Schindler M, Gärtner S, Pöhlmann S. 2019. Analysis
685 of IFITM-IFITM Interactions by a Flow Cytometry-Based FRET Assay. Int J Mol Sci 20.

686 47. Yount JS, Karssemeijer RA, Hang HC. 2012. S-Palmitoylation and Ubiquitination Differentially
687 Regulate Interferon-induced Transmembrane Protein 3 (IFITM3)-mediated Resistance to
688 Influenza Virus. J Biol Chem 287:19631–19641.

689 48. Chesarino NM, Compton AA, McMichael TM, Kenney AD, Zhang L, Soewarna V, Davis M,
690 Schwartz O, Yount JS. 2017. IFITM3 requires an amphipathic helix for antiviral activity. EMBO
691 Rep 18:1740–1751.

692 49. Qian J, Le Duff Y, Wang Y, Pan Q, Ding S, Zheng Y-M, Liu S-L, Liang C. 2015. Primate
693 lentiviruses are differentially inhibited by interferon-induced transmembrane proteins. Virology
694 474:10–18.

695 50. Ahi YS, Yimer D, Shi G, Majdoul S, Rahman K, Rein A, Compton AA. 2020. IFITM3 Reduces
696 Retroviral Envelope Abundance and Function and Is Counteracted by glycoGag. mBio 11.

697 51. Löytynoja A, Goldman N. 2008. Phylogeny-aware gap placement prevents errors in sequence
698 alignment and evolutionary analysis. Science 320:1632–1635.

699 52. Guindon S, Dufayard J-F, Lefort V, Anisimova M, Hordijk W, Gascuel O. 2010. New algorithms
700 and methods to estimate maximum-likelihood phylogenies: assessing the performance of
701 PhyML 3.0. Syst Biol 59:307–321.

53. Anisimova M, Gascuel O. 2006. Approximate likelihood-ratio test for branches: A fast, accurate, and powerful alternative. Syst Biol 55:539–552.

FIGURE LEGENDS

Figure 1. Presentation of the animal IFITMs used here. A) Schematic genomic organization of *IFITMs*. Black boxes indicate IFITMs that have been functionally analyzed here. Given that the anti-HIV-1 activities of human IFITM1, 2 and 3 have been well characterized, only human IFITM3 was used here as functional standard for the remaining IFITMs. B) Identity matrix of the different IFITMs. C) Comparison of the N and C termini of animal IFITMs. Left, Species cladogram. Right, Comparison of N and C terminal sequences of selected IFITMs. Nter sequences were aligned as described in Methods, while the Cter sequences have little sequence homology and are shown here as sequence list.

Figure 2. Confocal microscopy analysis of animal IFITMs. HEK293T cells ectopically transfected with DNAs coding the indicated IFITMs were fixed and analyzed by immunofluorescence and confocal microscopy analyses. The pictures are representative of the major distribution pattern observed by examining >50 positive cells per construct.

Figure 3. Mammalian IFITMs exhibit a broad functional heterogeneity in their ability to inhibit HIV-1 during either target cell protection or negative imprinting of virion particles infectivity. A) Schematic representation of the experimental system used here. To assess the activity of IFITMs in mediating the protection of target cells from infection, HEK293T cells were transiently transfected with plasmids coding CD4, CXCR4 and the indicated IFITMs. Cells were challenged 36 hours later with a GFP coding NL4-3-bearing HIV-1 vector for a single round of infection assay. The extent of infection was assessed by flow cytometry. To determine the ability of IFITMs to affect the infectivity of newly-

produced virion particles, HEK293T cells were instead transfected with DNAs coding the HIV-1 virus in addition to IFITMs. The amount of virion particles released in the supernatant was determined by exo-RT assay after ultracentrifugation through a 25% sucrose cushion. Virion infectivity was assessed after exo-RT normalization on HeLaP4 cells that stably express both CD4 receptor and CXCR4 co-receptor. The extent of infection was again assessed by flow cytometry. B) WB panels display representative results obtained when IFITMs were expressed in target cells (cell lysates, upper panels) or in virion-producing cells (purified virion particles, lower panels). C) Infectivities measured during target cell protection and negative imprinting of virion particles (avg, SEM $n \geq 4$; one-way Anova tests between the indicated conditions: only statistically significant p values are color-coded). D) Correlation between the two antiviral properties for each IFITM molecule: *, $p<0.0001$ following a Pearson's correlation coefficient analysis.

Figure 4. The steady state levels of the different IFITM proteins indicate a correlative, not absolute, trend between antiviral phenotype and levels of expression of IFITMs. Intracellular staining was used to measure the intracellular levels of IFITMs by flow cytometry in function of their MFI. A and B) Representative histograms and cumulative variations in the MFIs, in this case normalized to human IFITM3 (grey in the panels of A present staining of negative controls). Graphs present avg and SEM obtained from 3 independent experiments. C) Correlations between the antiviral effects of IFITMs and their intracellular accumulation levels. *: $p=0.0001$ (left) and $p=0.01$ (right), following a Pearson's correlation coefficient analysis between the indicated conditions.

751 **Figure 5. The phenotypic differences observed among selected IFITM molecules are**
752 **also governed by their intrinsic behavior and not only by protein stability.** Increasing
753 doses of the non-functional D1 and C1 IFITMs were compared to a fixed dose (starting from
754 equimolar to a 4-fold excess) of antiviral D1Lb and R1, respectively in target cell protection.
755 IFITM expressing cells were either analyzed by WB or challenged prior to flow cytometry
756 analysis three days later. IFITM levels were in this case measured by densitometry following
757 WB, as this yielded comparable results than intracellular staining and FACS. B) as in A, but
758 using decreasing doses of the antiviral R1 molecule, over a fixed dose of the non-functional
759 C1. Graphs present avg and SEM of at least 4 independent experiments and WB panels
760 present typical results obtained. *: $p<0.05$, following a one-tail Student t test between the
761 indicated conditions.
762
763 **Figure 6. Anti-viral and non-antiviral IFITMs do not present obvious distinguishing**
764 **marks.** A and B) Amino acid alignment of the tested IFITMs (A) and corresponding logo
765 plots (B) for the "Antiviral" and "Non-antiviral" (D3, C3, C1, and D1; highlighted in grey)
766 IFITMs, as described in this study. Grey underlines strictly non-antiviral IFITMs.
767 Visualization was performed with Geneious (Biomatters, Inc.), with color-coding according
768 to polarity. In panel A, H3 is set as the reference sequence; dots correspond to residues similar
769 to the reference sequence, while hyphens correspond to gaps. Numbering is according to H3
770 (human IFITM3) in panel A, and to the consensus sequence of the alignment in panel B. C)
771 Phylogenetic tree of the IFITMs tested here. Node supports are aLRT. The scale bar
772 represents number of amino acid substitutions per site.
773

Figure 7. A chimera approach between C1 and R1 IFITM proteins identifies the importance of the cross-talk between the TMD and the Cter domains for optimal antiviral activity. A) Schematic representation of the chimeras used. B and C) Western blot analysis and densitometric quantification following ectopic DNA transfection in HEK293T cells. D) Representative images of the intracellular distribution of the different chimeras obtained by confocal microscopy. E) Chimeras were tested in target cell protection by challenging HEK293T cells expressing the indicated chimeras thirty-six hours post DNA transfection with GFP-coding NL4-3-bearing HIV-1. The extent of infection was measured two days later by flow cytometry. The graphs present avg and SEM of at least 4 independent experiments and WB panels present typical results obtained. *: $p<0.05$, following a One-way Anova test between the indicated conditions.

Figure 8. D1/D1Lb chimeras further stresses the importance of the cross-talks between individual IFITM domains for optimal antiviral activity. As in the legend to figure 7. A) Schematic representation of the chimeras used. B and C) Western blot analysis and densitometric quantification following ectopic DNA transfection in HEK293T cells. D) Representative images of the intracellular distribution of the different chimeras obtained by confocal microscopy. E) Chimeras were tested in target cell protection by challenging HEK293T cells expressing the indicated chimeras thirty-six hours post DNA transfection with GFP-coding NL4-3-bearing HIV-1. The extent of infection was measured two days later by flow cytometry. The graphs present avg and SEM of at least 4 independent experiments and WB panels present typical results obtained. *: $p<0.05$, following a One-way Anova test between the indicated conditions.

Figure 9. Chimeras between C1/R1 and D1/D1Lb that are active for target cell protection conserve their ability to negatively imprint HIV-1 virions infectivity. A) Experimental scheme and chimeras tested here. B) Virions were produced in the presence of the indicated chimeras, normalized and used to challenge target cells. Infectivity was determined forty-eight hous later by flow cytometry. The graph presents avg and SEM of 3 independent experiments. *: $p<0.05$, following a One-way Anova test between the indicated conditions.

Figure 10. Murine IFITM3 intrinsically lacks the ability to negatively modulate the infectivity of newly-produced HIV-1 virion particles. A) Increasing doses of human and murine IFITM3s (H3 and M3, respectively) were used to produce HIV-1 particles and to determine whether M3 would hinge on HIV-1 virions infectivity. The panels and the graph present typical results obtained (n=3, avg and SEM). *: $p<0.05$, following a One-Way Anova test between the indicated conditions. B) The Y78F substitution was introduced in M3 and the mutant was tested for its ability to negatively imprint newly-produced HIV-1 virions. The panels and the graph present typical results obtained (n=3, avg and SEM). No statistically significant difference was observed between control and mutant.

A

INTERFERON-INDUCED TRANSMEMBRANE PROTEINS

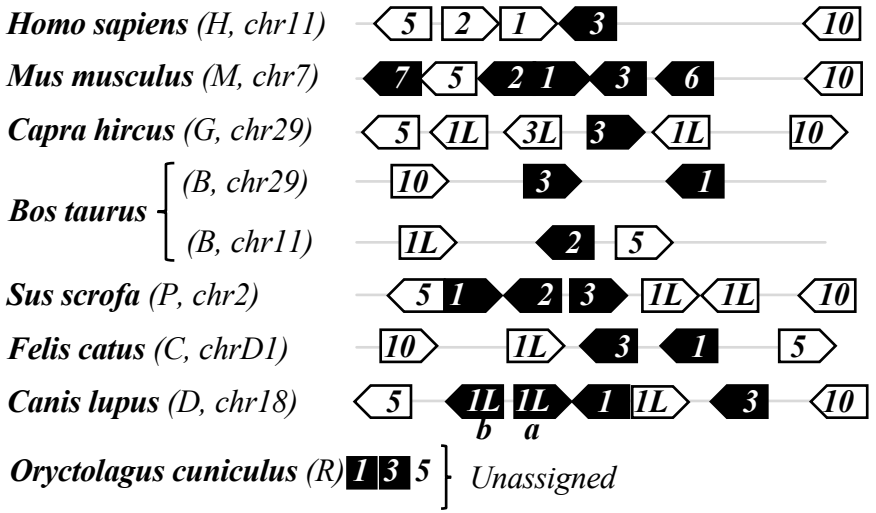

B

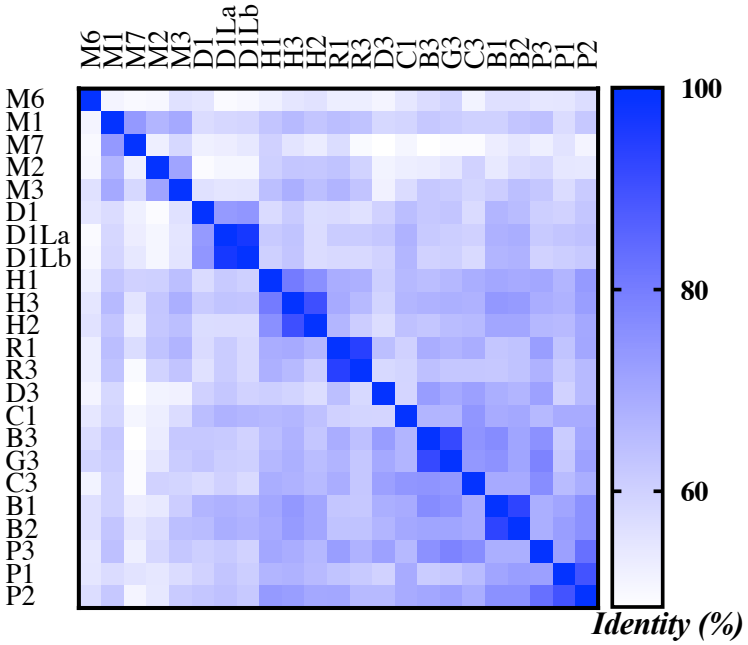

C

Domains

PPxY *(Nedd4)*

Yxxϕ *(AP2)*

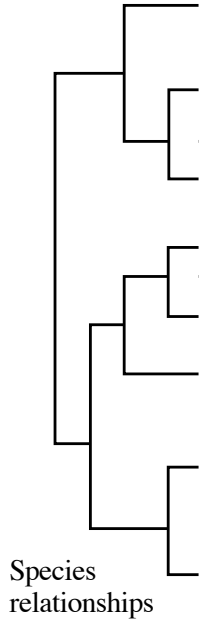

N-Term. **C-Term.**

```
H3   MNHTVQTFFSPVNSGQPPNYEMLKEEHEVAVLG-APHNPAPPTSTVIHIRSETSVPDH  IFQAYG
H2   MNHIVQT-FSPVNSGQPPNYEMLKEEQEVAMLG-VPHNPAPPMSTVIHIRSETSVPDH  VVQAQR
H1   ----------------------MHKEEHEVAVLG-APPSTILPRSTVINIHSETSVPDH  GSVTVYHIMLQIIQEKRGY
M3   MNHTSQAFITAASGGQPPNYERIKEEYEVAEMG-APHGSASVRTTVINMPREVSVPDH  IVLNAQNLHT
M2   MSHNSQAFLST-NAGLPPSYETIKEEYGVTELG-EPSNSAVVRTTVINMPREVSVPDH  TSVVVFQSFAQRTPHSGF
M1   ----------------------MPKEQQEVVVLG-SPHISTSATATTINMP-EISTPDH  R
R3   MSNVSKTFFSTASTSRTPNYEELREEHQIAVLG-APH-SAAVASTVINVHSEVSVPDH  SSAAIFHAISP
R1   ----------------------MSKEEHQVEMLG-APR-SAAVASTVINVHSEVSVPDH  SSAAIFHAISP
B3   MNRTSQPLFTGAHGAVPPAYEVLKEEHEVAVLG-APQSQAPLTTTVINIRSDTAVPDH  GSLMIVQAVSELMQNYGGH
B2   ----------------------MLKEENEVAVLG-APQSQAPVTTTVINIPRENSVPDH  VYMAAYETALRISRHGGH
B1   ----------------------MI-EEHEVAVLG-APQSQAPLTTTVINIRSDTAVPDH  VYMAAYETALRISRHGGH
G3   MNCTSQPLFTGAHGAVPPGYEVLKEEHEVAVLG-APQSPAPVTTTVINIRSDTAVPDH  GSLMIVQAILELIQNYGGH
P3   MNCASQPFFTGAHGG-PPTYEMLKEEHEVAVLG-APQTSAPVATTVINIRSETSVPDH  GSLVIFQAVLQLIKDYRGY
P2   MNCASQPFFTGAHGG-PPTYEMLKEEHEVAVLG-APQTSAPVATTVINIRSETSVPDH  VYITAYQMLERAKSNRGY
P1   MI-KSQ------H-------EM--D----G-LG-APQTSAPVATTVITIPRETSVPDH  VYITAYHMLERAKSNRGY
D3   MSRAPRPLLPGARAAGPPTYEMLKEEHEVVVLGGAPQSAAPATTTVINIRGDTVVPDH  GSLVIFETVSEMVKHYGGS
D1   ----------------------MDQDQYKVPETG-APQSMVPVTTTVINIRSDTVVPDH  AFGAAYWALLQVMQERSRYH
D1La ----------------------M-QN--KVDVRG-APLSTAPATTTVINVPVETVVPDH  AYAAAYGALLQAMQESGRYH
D1Lb ----------------------M-QN--KVDVRG-ALLSTAPATTTVINVPEETVVPDH  AYAAAYGALLQVMQESGRYH
C3   MNRNAQPFLPGTHTGVPPTYEMLKEEHEVAVLG-GPQSPAPMATTVINIQTETSVPDH  GSLVVFQAISEMMKGYGGY
C1   ----------------------MLKD-NKVDILE-GPQSSAPMATTVINIQTETSVPDH  AYLTAYSIILRVMQNSRGHH
```

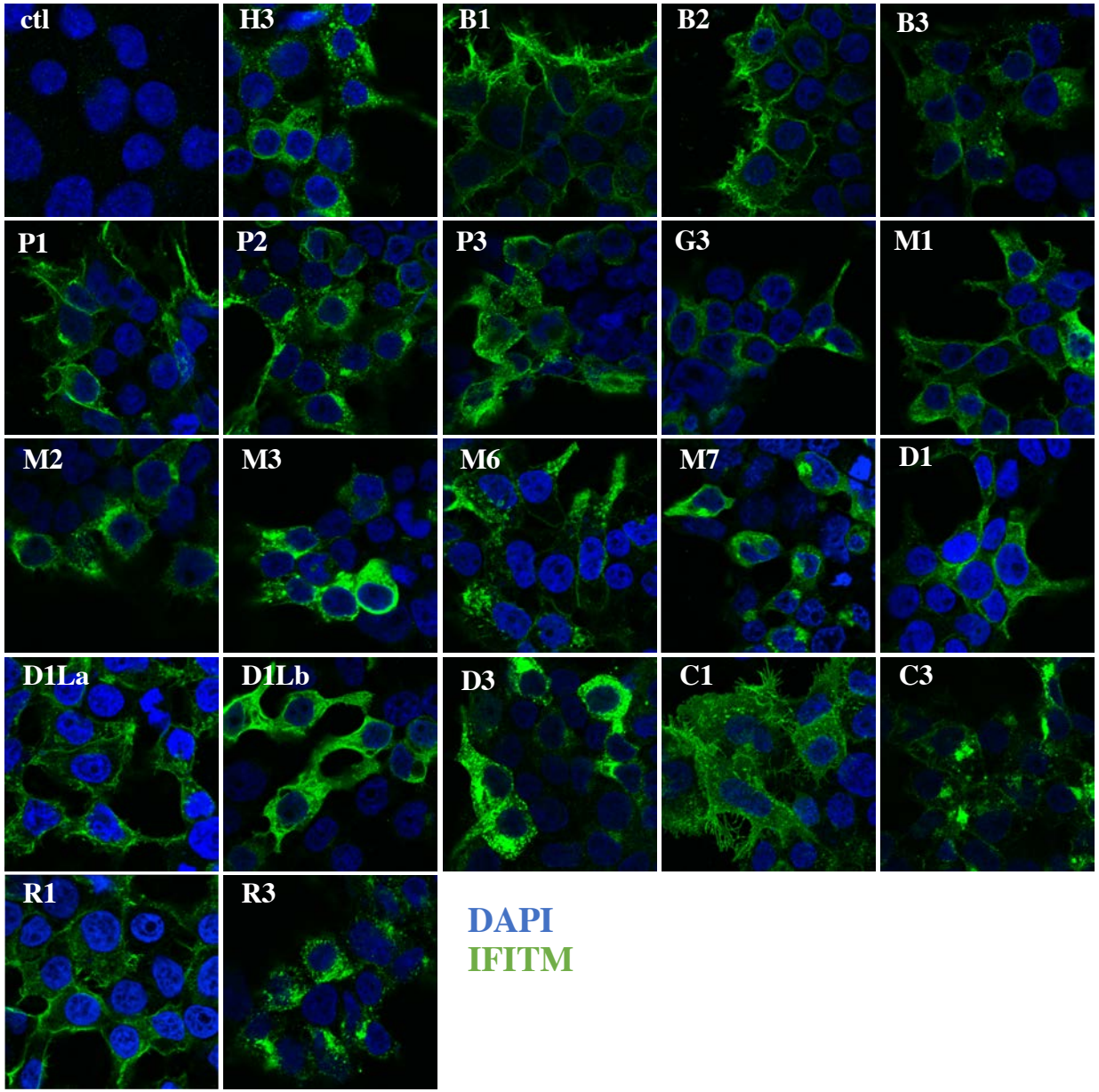
ctl
H3
B1
B2
B3
P1
P2
P3
G3
M1
M2
M3
M6
M7
D1
D1La
D1Lb
D3
C1
C3
R1
R3
DAPI
IFITM

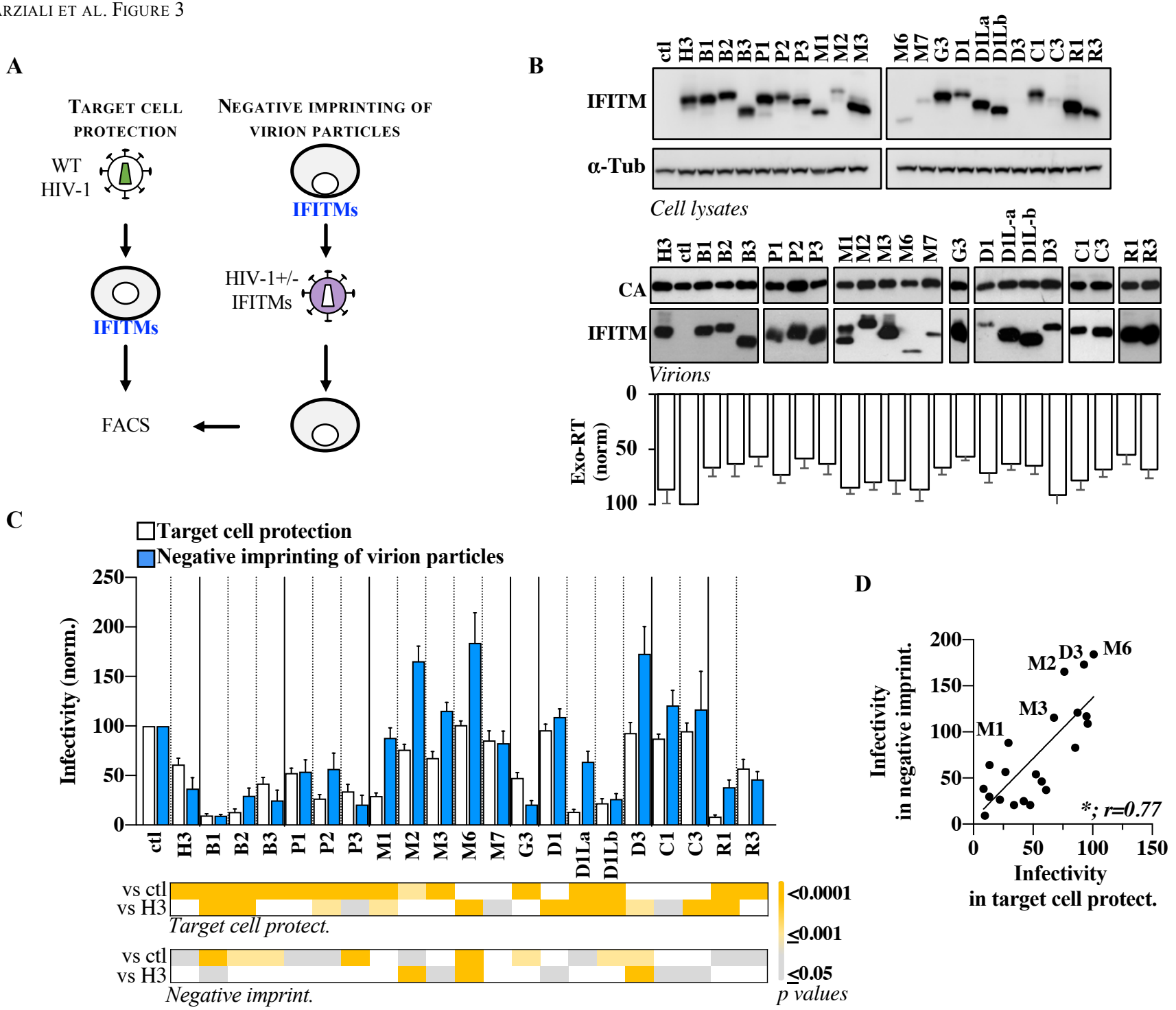
A
TARGET CELL PROTECTION
NEGATIVE IMPRINTING OF VIRION PARTICLES
WT HIV-1
IFITMs
HIV-1+/- IFITMs
IFITMs
FACS
B
ctl H3 B1 B2 B3 P1 P2 P3 M1 M2 M3 M6 M7 G3 D1 D1La D1Lb D3 C1 C3 R1 R3
IFITM
α-Tub
Cell lysates
H3 ctl B1 B2 B3 P1 P2 P3 M1 M2 M3 M6 M7 G3 D1 D1L-a D1L-b D3 C1 C3 R1 R3
CA
IFITM
Virions
Exo-RT (norm)
0
50
100
C
Target cell protection
Negative imprinting of virion particles
Infectivity (norm.)
250
200
150
100
50
0
ctl H3 B1 B2 B3 P1 P2 P3 M1 M2 M3 M6 M7 G3 D1 D1La D1Lb D3 C1 C3 R1 R3
vs ctl
vs H3
Target cell protect.
vs ctl
vs H3
Negative imprint.
≤0.0001
≤0.001
≤0.05
p values
D
Infectivity in negative imprint.
200
150
100
50
0
M6
D3
M2
M3
M1
*; r=0.77
0
50
100
150
Infectivity in target cell protect.

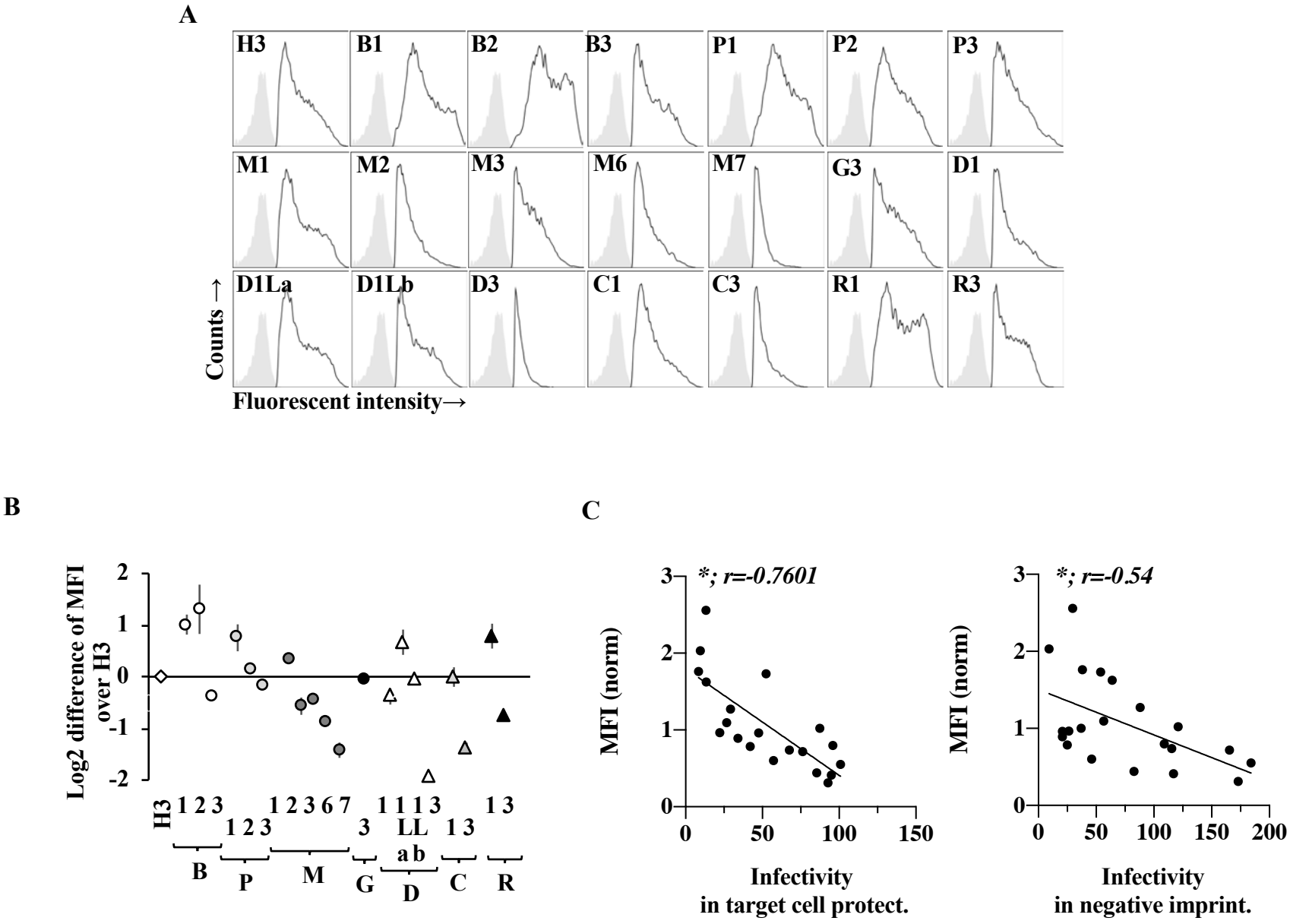
A
H3
B1
B2
B3
P1
P2
P3
M1
M2
M3
M6
M7
G3
D1
D1La
D1Lb
D3
C1
C3
R1
R3
Counts →
Fluorescent intensity→
B
Log2 difference of MFI over H3
2
1
0
-1
-2
H3 1 2 3 1 2 3 6 7 1 1 1 3 1 3
1 2 3 3 LL 1 3
a b
B
P
M
G
D
C
R
C
*; r=-0.7601
MFI (norm)
3
2
1
0
0 50 100 150
Infectivity
in target cell protect.
*; r=-0.54
MFI (norm)
3
2
1
0
0 50 100 150 200
Infectivity
in negative imprint.

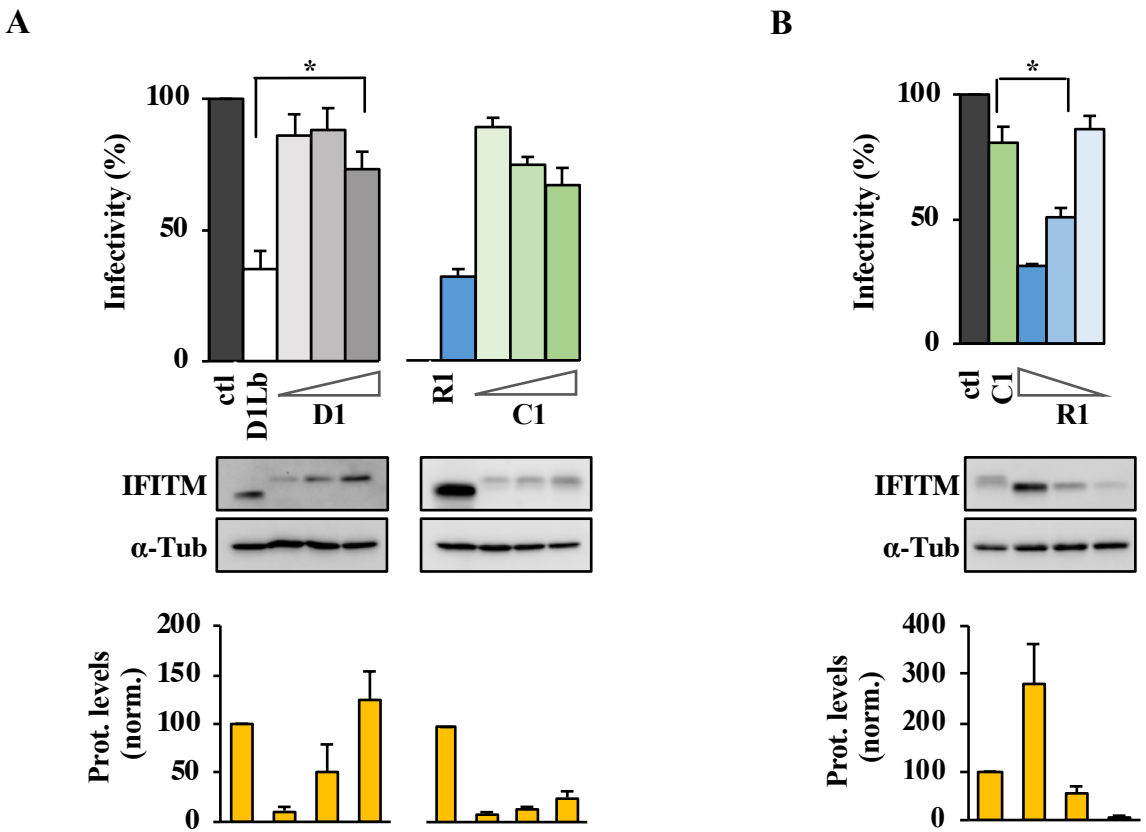
A
B
Infectivity (%)
100
50
0
*
ctl
D1Lb
D1
R1
C1
IFITM
α-Tub
Prot. levels (norm.)
200
150
100
50
0
400
300
200
100
0

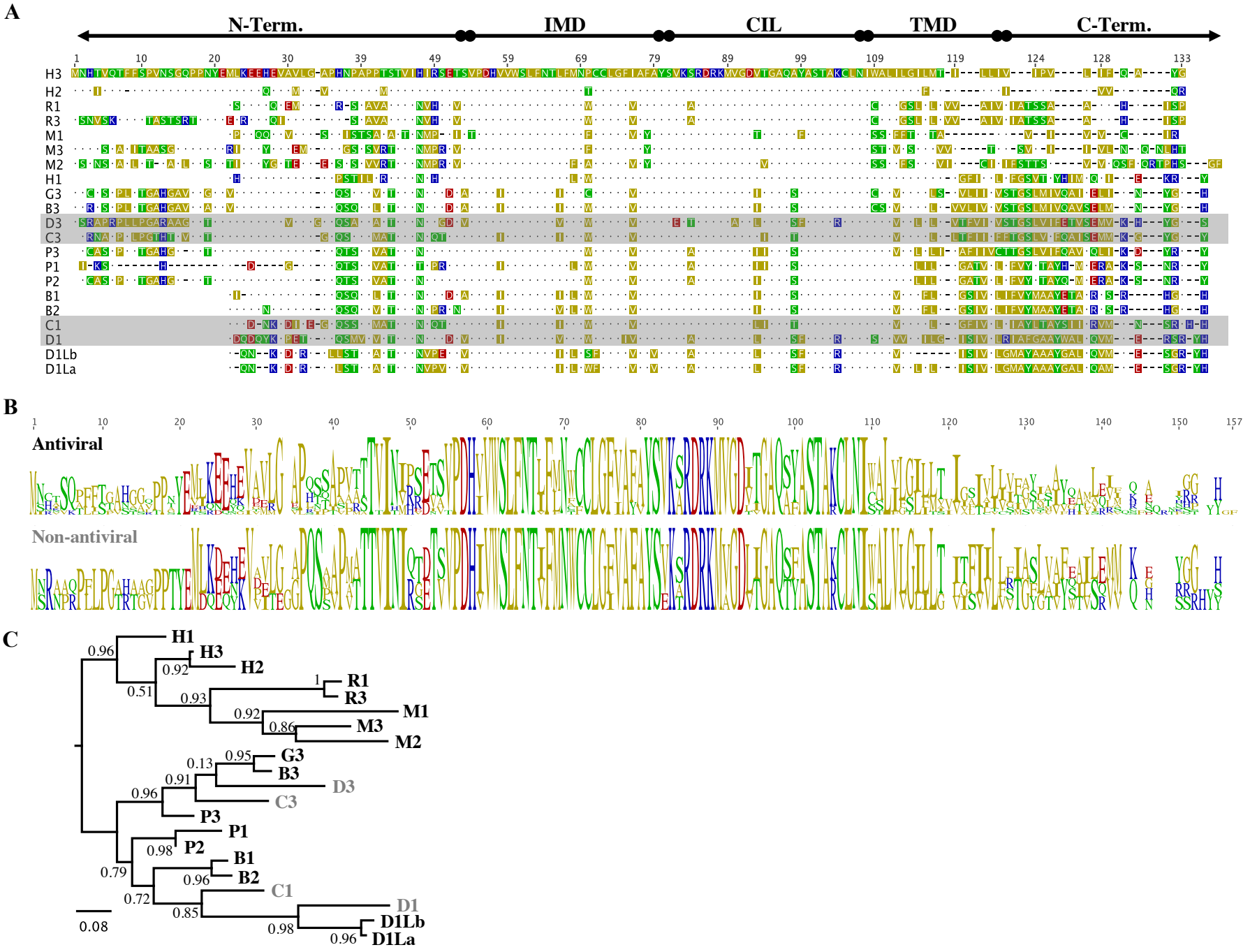
A
N-Term.
IMD
CIL
TMD
C-Term.
H3
H2
R1
R3
M1
M3
M2
H1
G3
B3
D3
C3
P3
P1
P2
B1
B2
C1
D1
D1Lb
D1La
B
Antiviral
Non-antiviral
C
H1
H3
H2
R1
R3
M1
M3
M2
G3
B3
D3
C3
P3
P1
P2
B1
B2
C1
D1
D1Lb
D1La
0.08

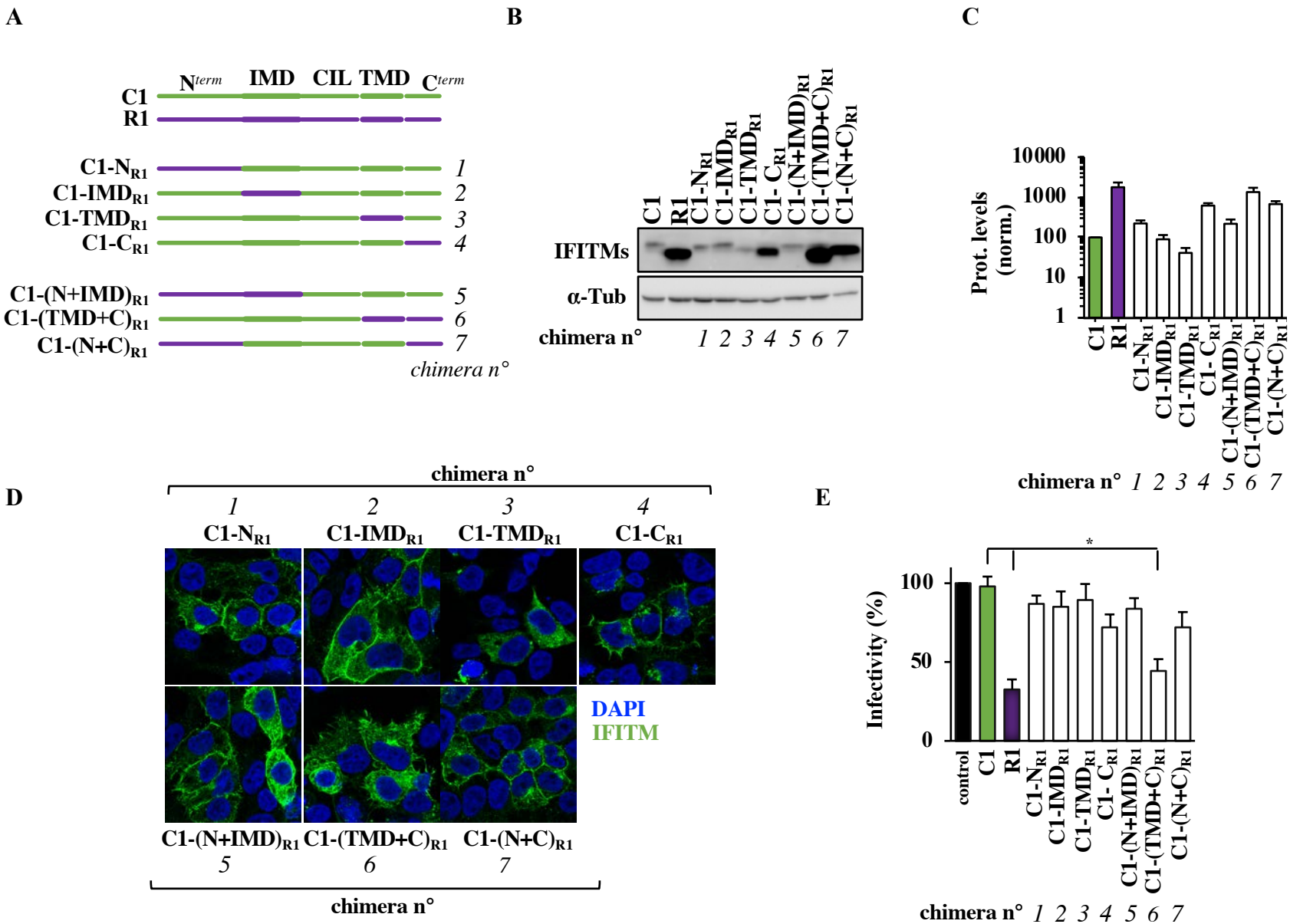
A
N^term
IMD
CIL
TMD
C^term
C1
R1
C1-N_R1
C1-IMD_R1
C1-TMD_R1
C1-C_R1
C1-(N+IMD)_R1
C1-(TMD+C)_R1
C1-(N+C)_R1
1
2
3
4
5
6
7
chimera n°
B
IFITMs
α-Tub
chimera n° 1 2 3 4 5 6 7
C
Prot. levels (norm.)
10000
1000
100
10
1
chimera n° 1 2 3 4 5 6 7
D
chimera n°
DAPI
IFITM
E
Infectivity (%)
100
50
0
*
control
chimera n° 1 2 3 4 5 6 7

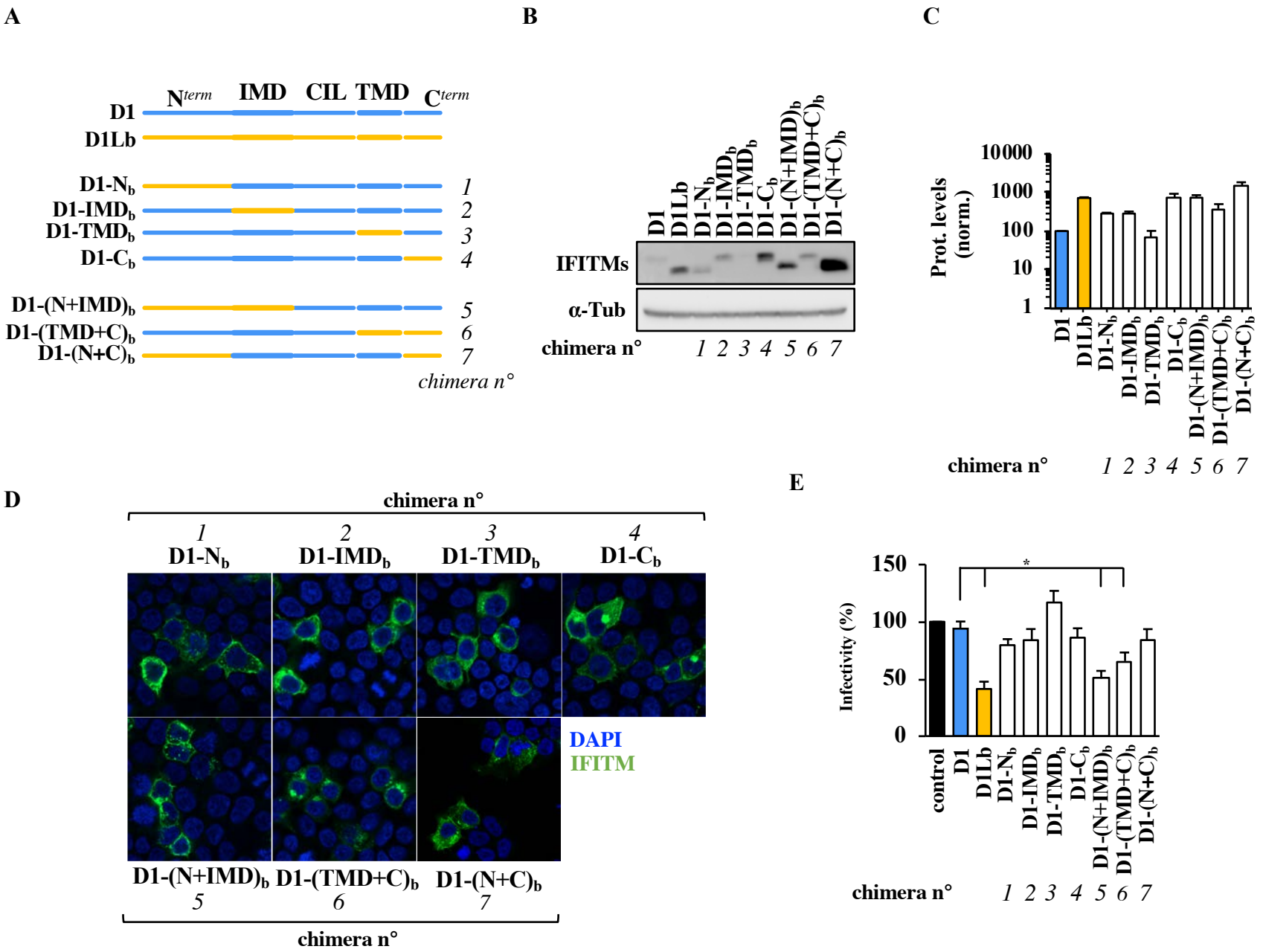
A
N^term
IMD
CIL
TMD
C^term
D1
D1Lb
D1-N_b
D1-IMD_b
D1-TMD_b
D1-C_b
D1-(N+IMD)_b
D1-(TMD+C)_b
D1-(N+C)_b
1
2
3
4
5
6
7
chimera n°
B
IFITMs
α-Tub
chimera n° 1 2 3 4 5 6 7
C
Prot. levels (norm.)
10000
1000
100
10
1
chimera n° 1 2 3 4 5 6 7
D
chimera n°
D1-N_b
D1-IMD_b
D1-TMD_b
D1-C_b
D1-(N+IMD)_b
D1-(TMD+C)_b
D1-(N+C)_b
DAPI
IFITM
E
Infectivity (%)
150
100
50
0
*
control
chimera n° 1 2 3 4 5 6 7

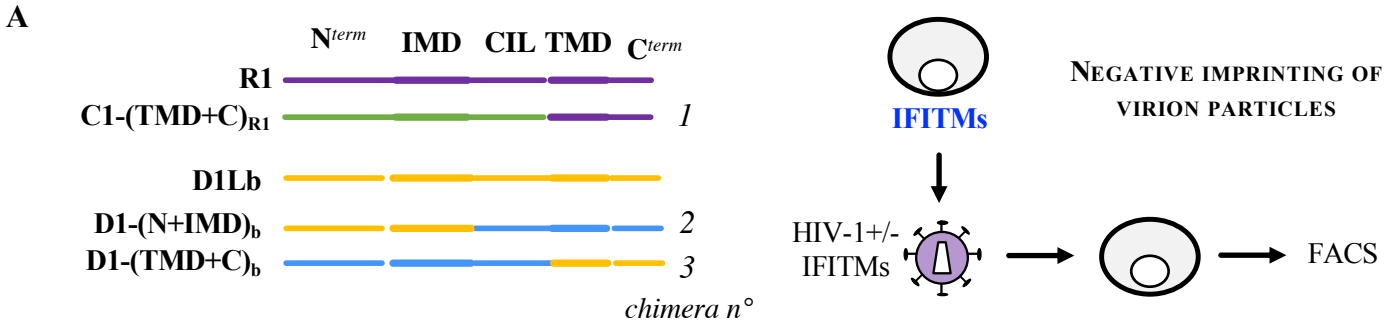
A
N^term
IMD
CIL
TMD
C^term
R1
C1-(TMD+C)R1
1
D1Lb
D1-(N+IMD)b
2
D1-(TMD+C)b
3
chimera n°
IFITMs
NEGATIVE IMPRINTING OF VIRION PARTICLES
HIV-1+/- IFITMs
FACS

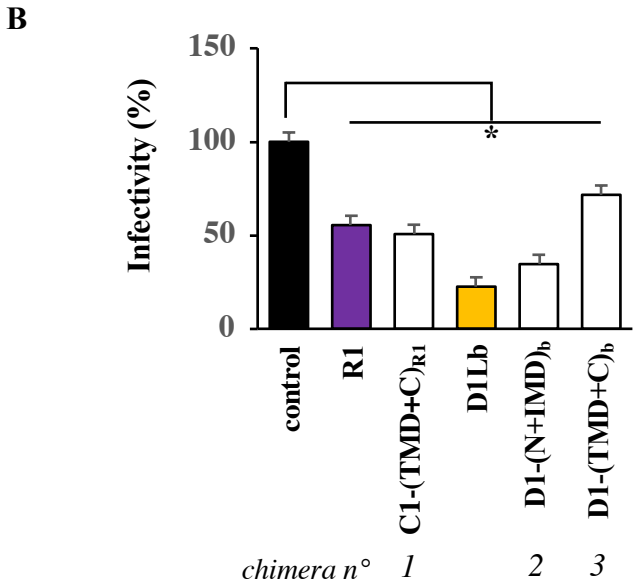
B
Infectivity (%)
150
100
50
0
*
control
R1
C1-(TMD+C)R1
D1Lb
D1-(N+IMD)b
D1-(TMD+C)b
chimera n°
1
2
3

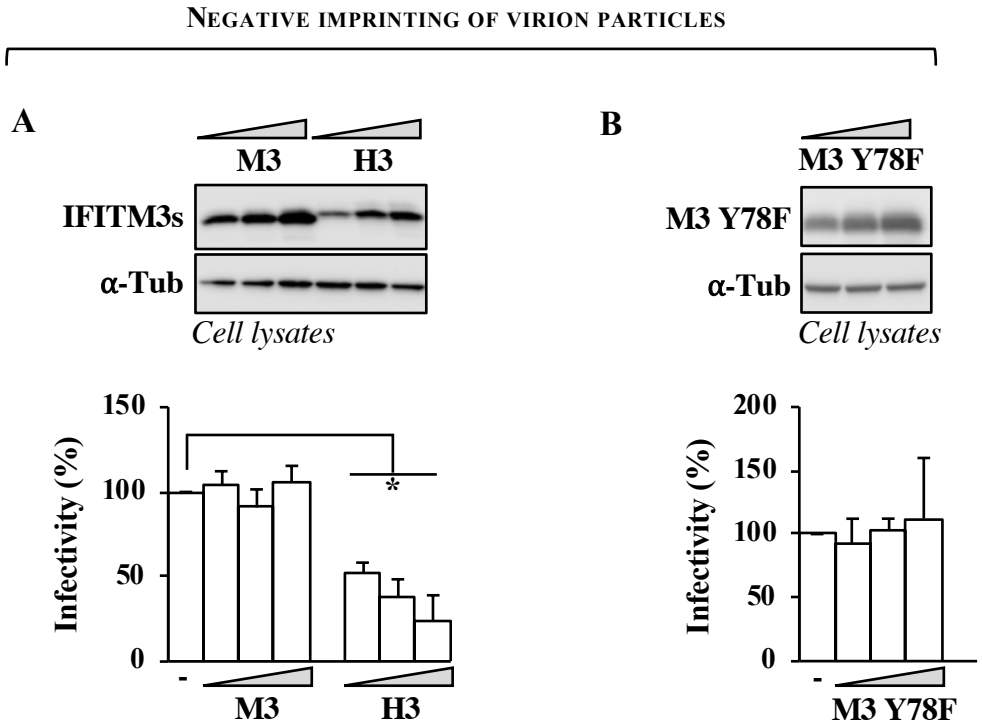
NEGATIVE IMPRINTING OF VIRION PARTICLES
A
M3
H3
IFITM3s
α-Tub
Cell lysates
Infectivity (%)
150
100
50
0
*
-
M3
H3
B
M3 Y78F
M3 Y78F
α-Tub
Cell lysates
Infectivity (%)
200
150
100
50
0
-
M3 Y78F